The Aeronautical Journal (2024), 1–18
doi:10.1017/aer.2024.61

RESEARCH ARTICLE

Optimal avoidance strategy based on nonlinear approximate analytic solution of non-cooperative differential game

S.J. Zhao, H.R. Zhang, R. Lyu, J. Yang and C.C. Xue

China Academy of Launch Vehicle Technology, Beijing, China
Corresponding author: Shenjia Zhao; Email: hehua88656@163.com

Received: 19 December 2023; **Revised:** 18 May 2024; **Accepted:** 28 May 2024

Keywords: aircraft evasion-pursuit game; non-cooperative differential game; Hamilton-Jacobi-Bellman equation; Cauchy initial value problem

Abstract

This study examines the pursuit-evasion game involving unmanned aerial vehicles (UAVs), with a specific focus on the scenario of N-pursuers-one-escapee. The primary objective is to develop an optimal strategy for the escapee when the pursuers possess superior capabilities. To obtain this objective, we conduct the following study. Firstly, to enhance realism, a non-cooperative differential game model is formulated, incorporating multiple motion characteristics, including aerodynamics, overloading, and imposed constraints. Secondly, the end-value performance index is subsequently converted to an integral one, simplifying the solution process of the Hamilton-Jacobi-Bellman (HJB) equation. An iterative method is utilised to determine the covariates using the Cauchy initial value problem, and its convergence and uniqueness are established. The optimal avoidance strategy is subsequently derived from the covariates. Finally, the superiority of the proposed strategy is validated through simulation experiments and compared to three advanced optimal avoidance strategies. A total of 1,000 anti-jamming simulation experiments are conducted to verify the robustness of the proposed strategy.

Nomenclature

x, y, z	the coordinates in the North Celestial Inertial System
V	the magnitude of velocity
D	the aerodynamic drag
L	the aerodynamic lift
m	the mass
g	the local gravitational acceleration
D_i, $(i = 1, 2)$	the i-th pursuer
M	the escapee
V_{Dmi}	the velocity projection of MD_i the firing plane of M
V_{Ddi}	the velocity projection of MD_i the firing plane of D_i
V_{Tmi}	the component of velocity of M in the horizontal plane
V_{Tdi}	the component of velocity of D_i in the horizontal plane
R_{Di}	the relative distance of the firing plane
$\bar{R}_{Di}$	the transformed relative distance of the firing plane
$\bar{R}_{Ti}$	the transformed relative distance of the horizontal plane
x_i	the relative velocity
f_{Di}	the MD_i of the firing plane system M control volume coefficient
g_{Di}	the MD_i of the firing plane system D control volume coefficient
h_{Di}	the MD_i of the firing plane system coefficient
f_{Ti}	the MD_i of the horizontal plane system M control volume coefficient

g_{Ti}	the MD_i of the horizontal plane system D control volume coefficient
h_{Ti}	the MD_i of the horizontal plane system coefficient
u_{Dm}	the firing plane control variable
u_{Tm}	the horizontal plane control variable
J	the perferomance index
t_{fi}	the terminal moment of MD_i
t_0	the initial time
l_i	the time operator
H	the Hamiltonian function
$p(t)$	the left term of the Cauchy's initial value equation
$q(t)$	the right term of the Cauchy's initial value equation
Q	the upper bound of $\left(\lvert I(q(x,t))\rvert + \int_t^{\frac{\bar{R}_i\beta_i+\bar{R}_{i0}\beta_{i0}}{}} l_i dt + 2\bar{R}_i\beta_i l_i\right)$
S	the upper bound of $\left\lvert \lambda_i^{(n)}(x,t) - \lambda_i^{(n-1)}(x,t)\right\rvert$
L	A sufficiently large constant (used in the Section 3.3.2)
N	A sufficiently large constant (used in the Section 3.3.3)
n	number of iterations

Greek symbol

Θ	the trajectory angle
Ψ	the trajectory yaw angle
ν	the velocity pitch angle
α	the angle-of-attack
λ_{Ti}	the line-of-sight azimuth
λ_{Di}	the line-of-sight elevation angle
ϕ_{Tmi}	the front angle of the horizontal plane of M
ϕ_{Dmi}	the front angle of the MD_i firing plane of M
ϕ_{Tdi}	the front angle of the horizontal plane of D_i
ϕ_{Ddi}	the front angles of the MD_i firing plane of D_i
γ_{Tmi}	the horizontal plane velocity angle of M
γ_{Dmi}	the firing plane velocity angle of M
γ_{Tdi}	the horizontal plane velocity angle of D_i
γ_{Ddi}	the firing plane velocity angle of D_i
α_{Di}	conversion factor
β_i	the weight of the terminal value index
β_{i0}	the initial weight of the terminal value index
κ_T	the weight of the energy metric
ϕ	Hamiltonian variation
λ_i	the covariant variable
ζ	the moment in (t, t_0) in proof of convergence
ξ	the moment in (t, t_0) in proof of uniqueness

1.0 Introduction

In a pursuit-evasion game, the escapee avoids the pursuer to reach a goal. Meanwhile, the pursuer aims to catch the escapee before it arrives. The escapee's situation changes over time, demanding a dynamic avoidance strategy. Differential games are often applied here. Problems vary, based on the number of players on each side. For example, there are games with one pursuer and one escapee, or with N pursuers and one escapee, or with N pursuers and N escapees. In a game with multiple players, the one-pursuer-multi-escapees scenario is the subject of concern. An example is the 'two cutters and a ship' game. Here, two fast pursuers team up to catch a slower escapee quickly. This game has sparked much research. Differential games have applications in economics, sports, robotics and air combat [1].

This study focuses on the best strategy for UAVs in pursuit-evasion games. It is important to note that the applications of these mathematical tools may not be suitable for the scenario. However, the motion

of the vehicle is non-linear and complex. Moreover, directly solving the joint multiple equations will lead to a dimensional disaster. Therefore, it highlights the growing in the optimal avoidance problem with nonlinear differential games for multiple vehicles in recent years [2, 3].

Existing studies often use linearisation and geometric methods to solve the optimal avoidance strategy of an escapee.

(1) Linearisation method: Solving the UAV's non-linear dynamic equations with Linear Quadratic Differential Game (LQDG) makes it simple [4–9]. However, the variable zero effort miss (ZEM), an important factor, only works for slower, closer scenarios [10–13]. LQDG uses a transfer matrix to solve ZEM, leading to large errors. Additionally, simplifying the evasion problem with many pursuers into a two-player game and merging strategies overlooks multiple interceptors' impact [14]. This, in turn, weakens the evasion effect.

(2) Geometric approach: The geometric approach uses Apollo circles [15], Tyson polygons [16] and the Voronoi diagram [17, 18] to define escapee and pursuer dominance zones. It also sets the boundary where they meet [19–22]. Geometric methods avoid nonlinear solution problems but assume uniform motion, a big limitation. Real-world relationships are complex and change. This flawlessly simplifies spatial relationships. However, it impacts the vehicle's evasion effectiveness.

Scholars have solved differential game problems using various methods. These include the viscous solution [23–25] and weak Kolmogorov-Arnold-Moser theory (KAM) theory [26], etc. S. Hamadene [27] proposed the solution of the mixed zero and stochastic differential game by applying the oriented stochastic differential equations with local solutions. Shipei [28] established a nonlinear parabolic variational inequality for the HJB equation under sufficiently smooth conditions, proving that the value function is the unique viscosity solution of its inequality with applications. However, the above mathematical derivation is valid under limited conditions, such as the time periodicity of the viscous solution [29], the control variable tends to 0, and so on. Therefore, a solution method with high applicability and low error is needed for the flying vehicle game problem

This paper suggests an optimal strategy for the 'N-pursuers-1-escapee' game. It is adapted to UAV dynamics. To obtain this strategy, we conduct the following study. First, a differential game model is constructed from the UAV's position-velocity relationship. Secondly, the final avoidance amount is taken as the performance index and converted to integral type to construct the Hamiltonian function to reduce the number of joint equations and avoid falling into dimensional catastrophe. Then, the covariates that satisfy the Cauchy initial value problem are constructed, and its convergence and uniqueness are proved. So the optimal avoidance strategy is obtained. Compared to three advanced optimal avoidance strategies, the simulation results show strong feasibility and robustness of the proposed strategy in this paper.

The contribution of this paper to the problem of pursuit-evasion game by UAVs can be summarised as follows:

(1) This method simplifies complex dynamics and finds a solution for vehicle games.
(2) It solves HJB system covariates. It works with the Cauchy problem, proving their convergence and uniqueness.

2.0 Problem description and modelling

2.1 Description of problems

This paper's research objects are both the escapee and pursuers. It focuses especially on the escapee. Its task is to avoid pursuit and reach its destination.

The confrontation scenario is shown in Fig. 1: M is the escapee, $D1$ and $D2$ are pursuers and T is M's destination.

Where λ_{D1}, λ_{D2} are the elevation angles of the line of sight, and λ_{T1}, λ_{T2} is the azimuth angle of the line of sight. Pursuers $D1$ and $D2$ pursue escapee M at different heights and directions, respectively. $S1$ and $S2$ are the target coordinate systems of $D1$ and $D2$.

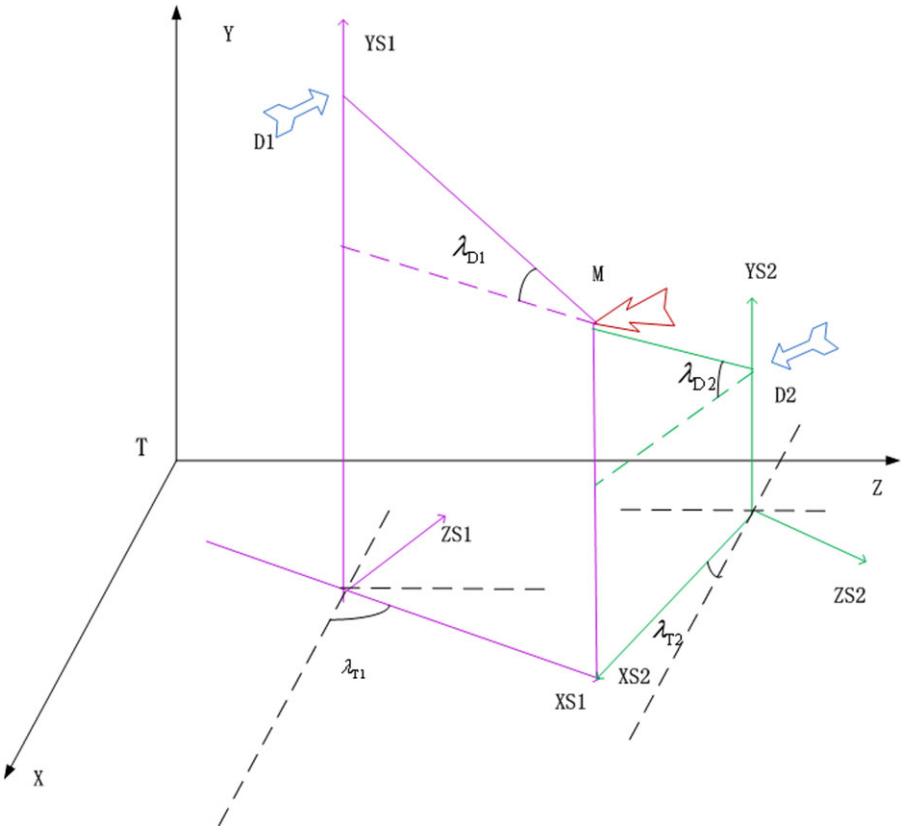

Figure 1. *Confrontation scenario.*

2.2 System model

2.2.1 dynamical model

The UAV dynamics are modeled as Equation (1):

$$\begin{cases} \dot{x} = V\cos\Theta\cos\Psi \\ \dot{y} = V\sin\Theta \\ \dot{z} = V\cos\Theta\sin\Psi \\ \dot{V} = -\dfrac{D}{m} - g\sin\Theta \\ \dot{\Theta} = \dfrac{L\cos\nu}{mV} - \dfrac{g\cos\Theta}{V} \\ \dot{\Psi} = \dfrac{L\sin\nu}{mV\cos\Theta} \end{cases} \tag{1}$$

Where V is the magnitude of velocity, Θ is the trajectory angle, Ψ is the trajectory yaw angle, x, y, z is the coordinates in the North Celestial Inertial System, D is the aerodynamic drag, L is the aerodynamic lift, ν is the velocity pitch angle, g is the local gravitational acceleration, and m is the mass.

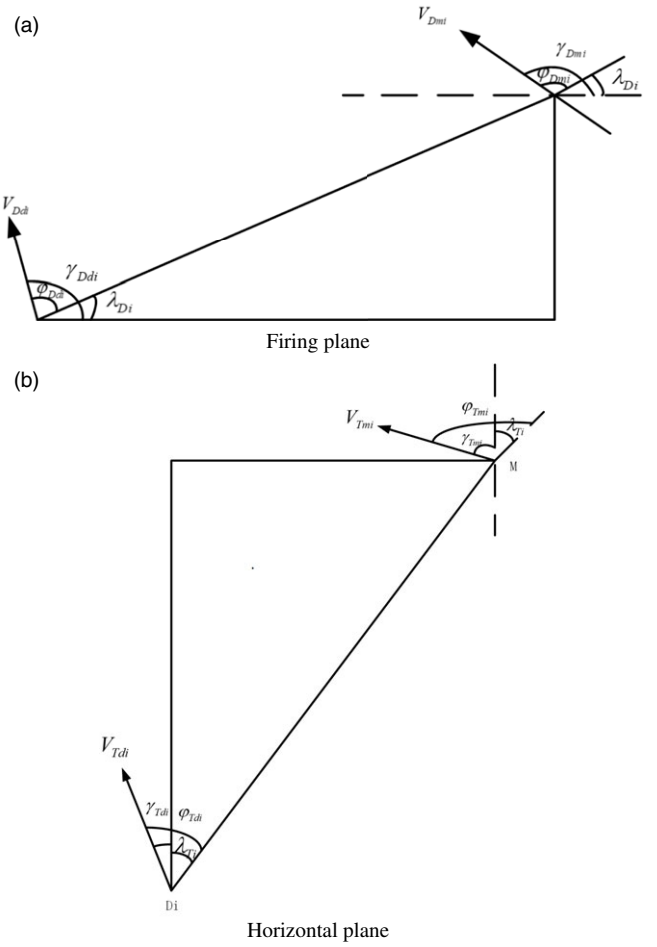

Figure 2. *Planar motion decoupling.*

2.2.2 Relative motion model

In the differential game model, we simplify the target coordinate system. First, we switch from the Northeastern system to the one in Fig. 1. It's split into the firing and horizontal planes, as shown in Fig. 2.

Where λ_{Di} is the line-of-sight elevation angle, V_{Dmi}, V_{Ddi} are the velocitys projection of the firing plane M and D_i, $(i = 1, 2)$, γ_{Dmi}, γ_{Ddi} are the firing plane velocity angles, ϕ_{Dmi}, ϕ_{Ddi} are the front angles of the firing planes of escapee M and pursuer D_i. λ_{Ti} is the line-of-sight azimuth, V_{Tmi}, V_{Tdi} are the velocity projections of M and $D_i(i = 1, 2)$ in the horizontal plane, γ_{Tmi}, γ_{Tdi} are the horizontal plane velocity angles, and ϕ_{Tmi}, ϕ_{Tdi} are the front angles of the horizontal plane M and $D_i(i = 1, 2)$.

Modeling of relative motion in the firing plane is as Equation (2):

$$\begin{cases} \phi_{Dmi} = \gamma_{Dmi} - \lambda_{Di} \\ \phi_{Ddi} = \gamma_{Ddi} - \lambda_{Di} \\ \dot{R}_{Di} = V_{Dmi}\cos\phi_{Dmi} - V_{Ddi}\cos\phi_{Ddi} \\ R_{Di}\dot{\lambda}_{Di} = V_{Dmi}\sin\phi_{Dmi} - V_{Ddi}\phi_{Ddi} \end{cases} \tag{2}$$

Where R_{Di} is the distance between M and $D_i(i = 1, 2)$.

Let $\frac{V_{Dm1}}{V_{Dd1}} = \alpha_{D1}$, $\frac{V_{Dm2}}{V_{Dd2}} = \alpha_{D2}$, then let the transformed relative distance be as Equation (3):

$$\begin{cases} \bar{R}_{D1} = \alpha_{D1} \cos \phi_{Dm1} - \cos \phi_{Dd1} \\ \bar{R}_{D2} = \alpha_{D2} \cos \phi_{Dm2} - \cos \phi_{Dd2} \end{cases} \tag{3}$$

Let the transformed relative distance $\bar{R}_{D1}, \bar{R}_{D2}$ be the state variable x_1, x_2 for the differential game model and the angular velocity of the plane $\dot{\gamma}_{Dmi}$, $\dot{\gamma}_{Ddi}$ be the control variable u_{Dmi}, u_{Ddi}, then the system state is as Eqaution 4:

$$\begin{cases} \dot{x}_1 = f_{D1}(x,t)u_{Dm1} + g_{D1}(x,t)u_{Dd1} + h_{D1}(x,t) \\ \dot{x}_2 = f_{D2}(x,t)u_{Dm2} + g_{D2}(x,t)u_{Dd2} + h_{D2}(x,t) \end{cases} \tag{4}$$

Where $f_{Di}(x,t) = -\alpha_{Di} \sin \phi_{Dmi}$, $g_{Di}(x,t) = \sin \phi_{Ddi}$, $h_{Di}(x,t) = \dot{\lambda}_{Di} (\alpha_{Di} \sin \phi_{Dmi} - \sin \phi_{Ddi})$, $(i = 1, 2)$.

$\dot{\gamma}_{Dmi}$ are synthesised as the total firing plane control variable as the angular velocity command u_{Dm} for the trajectory angle, i.e., $\dot{\Theta} = u_{Dm}$. The same is true for the horizontal plane. But, the control variable there is the angular velocity command for the trajectory yaw, so $\dot{\Psi} = u_{Tm1} = u_{Tm2} = u_{Tm}$. The control variable in the horizontal plane is the angular velocity command for the trajectory yaw.

Combining Equation (1) gives the lift as Equation (5):

$$L = \sqrt{(mVu_{Dm} + mg \cos \Theta)^2 + (mV \cos \Theta u_{Tm})^2} \tag{5}$$

The overload is $N = \frac{L}{mg}$, and after the overload constraint, the real aerodynamic lift L and aerodynamic drag D are obtained using atmospheric interpolation, and the real trajectory angular velocity $\dot{\Theta}$ and trajectory yaw angular velocity $\dot{\Psi}$ are obtained from Equation (1).

3.0 Non-cooperative differential game optimal avoidance strategy design

This section solves the problem of avoiding two pursuers in the UAV pursuit-evasion scenario. The solution revolves around a function and key variables. The study introduces a new method for solving complex differential games. It directly uses three-degree-of-freedom equations. First, it sets up a performance index to manage the game dynamics. Then, it creates a Hamiltonian function. This function is derived from the initial index. It determines the best control variable with the covariate. The study then introduces a fresh approach. It integrates the Cauchy initial value problem. This integration helps to systematically derive solutions for the variables. The paper also proves the convergence and uniqueness of these solutions. This work improves the practical and theoretical strategies for UAV evasion.

The process is illustrated in Fig. 3.

Where *um* is the optimal avoidance strategy for UAV.

3.1 Performance indicators

The firing plane and the horizontal plane are decoupled. From the perspective of evasion, the horizontal plane is taken as an example, and the design performance index is:

$$\min_{u_{Tm}} J = -\frac{1}{2}\beta_1 (t_{f1}) \bar{R}_{T1}^2 (t_{f1}) - \frac{1}{2}\beta_2 (t_{f2}) \bar{R}_{T2}^2 (t_{f2}) + \frac{1}{2}\kappa_T \int u_{Tm}^2 dt \tag{6}$$

Where $\beta_i(t) = \frac{V_{Tdi}(t)}{V_{d1}(t)+V_{d2}(t)}$ is the weight of the terminal value index, t_{fi} $(i = 1, 2)$ is the terminal moment and $\bar{R}_{T1}, \bar{R}_{T2}$ is the transformed relative distance from the escapee and pursuer on the horizontal plane corresponding to the transformation in (3). κ_T is the weight of the energy metric.

The performance index aims to increase the distance between the escapee and pursuer. It also aims to reduce the escapee's energy use. This index shows the evasion and energy. The parameter $\beta_i(t)$ is modifiable to dynamically adjust according to the capabilities of the pursuer, thereby augmenting the significance of the threat of a proficient pursuer. This adaptive mechanism serves to mitigate the inherent

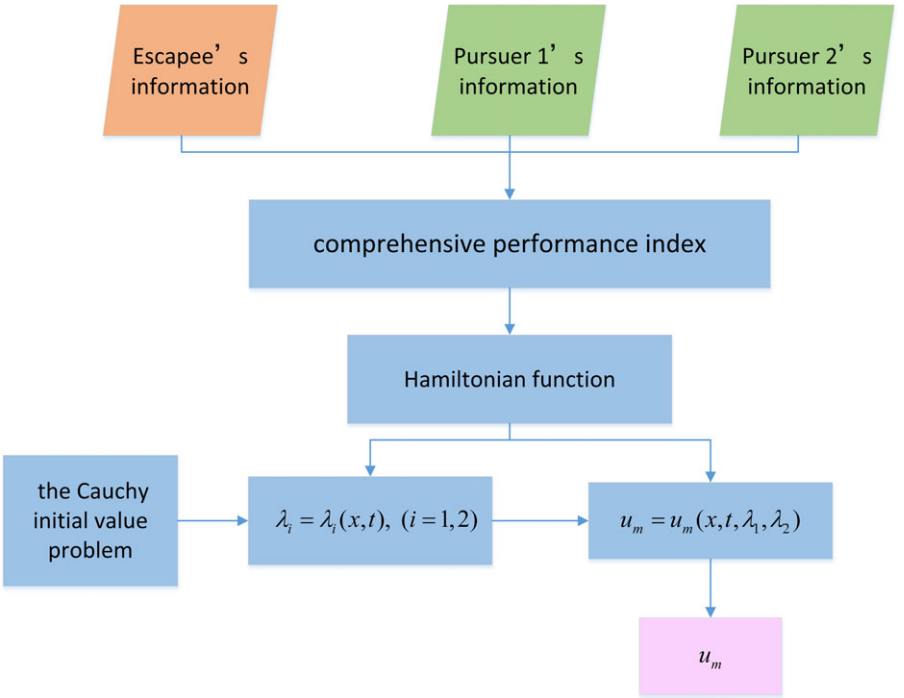

Figure 3. *Process.*

limitation of relying solely on distance metrics for evaluating the dynamics of the game. Parameter κ_T based on engineering experience.

To represent the amount of last-minute avoidance, which can't be estimated or predicted, it is converted to an integral index [30]:

$$\begin{aligned}\frac{1}{2}\beta_i\bar{R}_{Ti}^2\left(t_{fi}\right) &= \frac{1}{2}\beta_{i0}\bar{R}_{Ti}^2\left(t_0\right) + \frac{1}{2}\int_{t_0}^{t_{fi}} d\left(\beta_i\bar{R}_{Ti}^2\right)dt \\ &= \frac{1}{2}\beta_{i0}\bar{R}_{Ti}^2\left(t_0\right) + \int_{t_0}^{t_{fi}}\left(\beta_i x_i\bar{R}_{Ti} + \frac{1}{2}\dot{\beta}_i\bar{R}_{Ti}^2\right)dt\end{aligned} \tag{7}$$

Thereby the performance index is converted to:

$$\begin{aligned}\min_{u_{Tm}} J = &-\frac{1}{2}\beta_{10}\bar{R}_{T10}^2 - \frac{1}{2}\beta_{20}\bar{R}_{T20}^2 - \int_{t_0}^{t_f}\left[l_1\left(\beta_1 x_1\bar{R}_{T1}^2 + \frac{1}{2}\dot{\beta}_1\bar{R}_{T1}^2\right)\right. \\ &\left. + l_2\left(\beta_2 x_2\bar{R}_{T2}^2 + \frac{1}{2}\dot{\beta}_2\bar{R}_{T2}^2\right)\right]dt + \kappa_T\int_{t_0}^{t_f}\frac{1}{2}u_T^2 dt\end{aligned} \tag{8}$$

where β_{10}, β_{20} is the value of β_1, β_2 taken at the initial moment and $\bar{R}_{T10}, \bar{R}_{T20}$ the initial distance between the escapee M and the pursuer $D_i(i=1,2)$ after the transformation. $t_f = \max\{t_{f1}, t_{f2}\}$. $l_1 = \begin{cases}1, & t < t_{f1}\\ 0, & t \geqslant t_{f1}\end{cases}, l_2 = \begin{cases}1, & t < t_{f2}\\ 0, & t \geqslant t_{f2}\end{cases}$ are the time operators.

This procedural change streamlines the solution process. It maintains the integrity of the solution and avoids adding errors.

3.2 HJB equations solving

The Hamiltonian function is:

$$\begin{aligned} H = &-l_1\left(\beta_1 x_1 \bar{R}_{T1} + \frac{1}{2}\dot{\beta}_1 \bar{R}_{T1}^2\right) - l_2\left(\beta_2 x_2 \bar{R}_{T2} + \frac{1}{2}\dot{\beta}_2 \bar{R}_{T2}^2\right) + \frac{1}{2}\kappa_T u_{Tm}^2 \\ &+ \lambda_1(f_{T1}(x,t)u_{Tm} + g_{T1}(x,t)u_{Td1} + h_{T1}(x,t)) \\ &+ \lambda_2(f_{T2}(x,t)u_{Tm} + g_{T2}u_{Td2} + h_{T2}(x,t)) \end{aligned} \tag{9}$$

According to the reference [31], let the

$$\begin{aligned} \phi = &-l_1\left(\beta_1 x_1 \bar{R}_{T1}^2 + \frac{1}{2}\dot{\beta}_1 \bar{R}_{T1}^2\right) - l_2\left(\beta_2 x_2 \bar{R}_{T2} + \frac{1}{2}\dot{\beta}_2 \bar{R}_{T2}^2\right) \\ &+ \frac{1}{2}\kappa_T u_{Tm}^2 + \lambda_1(f_{T1}(x,t)u_{Tm}) + \lambda_2(f_{T2}(x,t)u_{Tm}) \end{aligned} \tag{10}$$

Where u_{Tm} reaches the optimal solution.

$$\frac{\partial \phi}{\partial u_{Tm}} = \frac{-l_1\left(\beta_1 x_1 \bar{R}_{T1}^2 + \frac{1}{2}\dot{\beta}_1 \bar{R}_{T1}^2\right) - l_2\left(\beta_2 x_2 \bar{R}_{T2} + \frac{1}{2}\dot{\beta}_2 \bar{R}_{T2}^2\right)}{\partial u_{Tm}} + \kappa_T u_{Tm} + \lambda_1(f_{T1}(x,t)) + \lambda_2(f_{T2}(x,t)) \tag{11}$$

Taylor expands $\overline{R_i}, x_i$ to obtain

$$\begin{cases} \bar{R}_i = \bar{R}_{i0} + x_i t + \frac{1}{2}\dot{x}_i t^2 + o(t^3) \\ x_i = x_{i0} + \dot{x}t + o(t^2) \end{cases} \tag{12}$$

solving for u_{Tm} is

$$\begin{aligned} u_{Tm} = &\frac{1}{\kappa_T}\left(\beta_1 f_{T1}(x,t)\bar{R}_1 l_1 t + \frac{1}{2} f_{T1}(x,t)\left(\dot{\beta}_1 \bar{R}_1 + \beta_1 x_1\right) l_1 t^2 + \beta_2 f_{T2}(x,t)\bar{R}_2 l_2 t\right. \\ &\left. + \frac{1}{2} f_{T2}(x,t)\left(\dot{\beta}_2 \bar{R}_2 + \beta_2 x_2\right) l_2 t^2\right) - (\lambda_1 f_{T1}(x,t) + \lambda_2 f_{T2}(x,t)) \end{aligned} \tag{13}$$

3.3 Solving for covariates using Cauchy's initial value

3.3.1 Iterative solution method

Using the regular equation, Equation (14) is obtained:

$$\begin{cases} \dot{\lambda}_1(x,t) = -\dfrac{\partial H}{\partial x_1} = \beta_1 \bar{R}_1 l_1 \\ \dot{\lambda}_1(x,t) = -\dfrac{\partial H}{\partial x_1} = \beta_1 \bar{R}_1 l_1 \end{cases} \tag{14}$$

Let $\dot{\lambda}_i(x,t_0) = \beta_0 \bar{R}_{i0}$, from Equation (12), and Equation (14) we know that

$$\dot{\lambda}_i = \beta_i l_i\left(\bar{R}_{i0} + x_i t + \frac{1}{2}\dot{x}_i t^2, \ddot{\lambda}_i = \beta_i l_i (x_i + \dot{x}_i t)\right) \tag{15}$$

Then, the Cauchy initial value problem is satisfied:

$$\ddot{\lambda}_i + p(t)\dot{\lambda}_i = q_i(x,t) \tag{16}$$

Where $p(t) = \frac{2}{t}$, $q_i(x,t) = -\beta_i l_i\left(x_i + \frac{2\bar{R}_{i0}}{t}\right)$ $(i = 1, 2)$.

Referring to the reference (32), it is deduced that:

$$\lambda_i(x,t) = \frac{1}{p(t)}\left(I(q_i(x,t)) + I(\lambda_i(x,t)\dot{p}(t)) - \dot{\lambda}_i(x,t) + \beta_{i0}\bar{R}_{i0}\right) \tag{17}$$

An iterative approach was used to calculate $\lambda_i(x,t)$

$$\begin{cases} \lambda_i^{(n)}(x,t) = \dfrac{1}{p(t)}\left(I(q_i(x,t)) + I\left(\lambda_i^{(n-1)}(x,t)\dot{p}(t)\right) - \dot{\lambda}_i(x,t) + \beta_{i0}\bar{R}_{i0}\right) \\ \lambda^{(0)}(x,t) = -\dfrac{t}{2}\left(\bar{R}_i\beta_i + \beta_{i0}\bar{R}_{i0}\right) l_i \end{cases} \tag{18}$$

Taking the value of the 5th iteration, λ_i is obtained:

$$\begin{aligned} \lambda_i = l_i\Bigg(&\frac{1}{48}\bar{R}_{i0}\beta_{i0}t\ln^4 t + \frac{1}{48}\bar{R}_i\beta_i t\ln^4 t - \frac{1}{6}\bar{R}_i\beta_i t\ln^3 t + \frac{1}{6}\bar{R}_{i0}\beta_{i0}t\ln^3 t \\ &+ \frac{1}{6}\bar{R}_{i0}\beta_i\ln^3 t + \frac{1}{2}\bar{R}_i\beta_i t\ln^2 t - \frac{1}{4}\bar{R}_{i0}\beta_{i0}t\ln^2 t + \frac{1}{2}\bar{R}_{i0}\beta_i t\ln^2 t \\ &-\bar{R}_i\beta_i t\ln t + \frac{1}{2}\bar{R}_{i0}\beta_{i0}t\ln t + \bar{R}_{i0}\beta_i t\ln t + \bar{R}_i\beta_i t - \frac{1}{2}\bar{R}_{i0}\beta_{i0}t\Bigg) \end{aligned} \tag{19}$$

3.3.2 Proof of convergence

From Equation (18), we know that

$$\lambda_i^{(n)}(x,t) - \lambda_i^{(n-1)}(x,t) = \frac{1}{p(t)}\left(I\left(\lambda^{(n-1)}(x,t)\dot{p}(t)\right) - I\left(\lambda_i^{(n-2)}(x,t)\dot{p}(t)\right)\right) \tag{20}$$

When n = 1, from Equations (17) and (18):

$$\begin{aligned} \lambda_i^{(1)}(x,t) - \lambda_i^{(0)}(x,t) &= \frac{1}{p(t)}[I(q(x,t)) + I\left(\lambda_i^{(0)}(x,t)\dot{p}(t)\right) - 2\bar{R}_i\beta l_i \\ &= -\frac{t}{2}\left[I(q(x,t)) - \int \frac{\bar{R}_i\beta_i + \bar{R}_{i0}\beta_{i0}}{t} l_i dt - 2\bar{R}_i\beta_i l_i\right] \end{aligned} \tag{21}$$

Since $\bar{R}_i, \bar{R}_{i0}, \beta_i, \beta_{i0} > 0, t_0 > 0, 0 < t < t_f$ and x_i, $\frac{2\bar{R}_{i0}}{t}$ are bounded, Equation (22) is deflated to obtain

$$\left|\lambda_i^{(1)}(x,t) - \lambda_i^{(0)}(x,t)\right| \le \frac{t}{2}\left(|I(q(x,t))| + \int \frac{\bar{R}_i\beta_i + \bar{R}_{i0}\beta_{i0}}{t} l_i dt + 2\bar{R}_i\beta_i l_i\right) \le Qt \tag{22}$$

where Q is the upper bound of $\left(|I(q(x,t))| + \int \frac{\bar{R}_i\beta_i + \bar{R}_{i0}\beta_{i0}}{t} l_i dt + 2\bar{R}_i\beta_i l_i\right)$

When $n = 2$, from Equation (18):

$$\left|\lambda_i^{(2)}(x,t) - \lambda_i^{(1)}(x,t)\right| = \left|\frac{1}{p(t)}(I)\,)\lambda_i^{(1)}(x,t) - \lambda_i^{(0)}(x,t))\dot{p}(t))\right| \le \left|-\frac{t}{2}\cdot Qt\int \frac{2}{t^2}dt\right| = Qt \tag{23}$$

When $n = 3$, from Equations (18) and (23):

$$\left|\lambda_i^{(3)}(x,t) - \lambda_i^{(2)}(x,t)\right| = \left|\frac{1}{p(t)}\left(I((\lambda_i^{(2)}(x,t) - \lambda_i^{(1)}(x,t))\dot{p}(t))\right)\right| \le Qt \tag{24}$$

And so on to get $\left|\lambda_i^{(n)}(x,t) - \lambda_i^{(n-1)}(x,t)\right| \le Qt$, so $\left|\lambda_i^{(n)}(x,t) - \lambda_i^{(n-1)}(x,t)\right|$ bounded.

When $n \geqslant 3$,

$$\begin{aligned} \lambda_i^{(n)}(x,t) - \lambda_i^{(n-1)}(x,t) &= \frac{1}{p(t)}\left(I\left(\lambda_i^{(n-1)}(x,t)\dot{p}(t)\right) - I\left(\lambda_i^{(n-2)}(x,t)\dot{p}(t)\right)\right) \\ &= \frac{1}{p(t)}\left(p(t)\left(\lambda_i^{(n-1)}(x,t) - \lambda_i^{(n-2)}(x,t)\right)\right) \\ &\quad - \frac{1}{p(t)}\int\left(\frac{1}{p(t)}\right)'\dot{p}(t)\left(\lambda_i^{(n-2)}(x,t) - \lambda_i^{(n-3)}(x,t)\right)p(t)dt \\ &= \left(\lambda_i^{(n-1)}(x,t) - \lambda_i^{(n-2)}(x,t)\right) + \frac{t}{2}\int\frac{2}{t^3}\left(\lambda_i^{(n-2)}(x,t) - \lambda_i^{(n-3)}(x,t)\right)dt \end{aligned} \tag{25}$$

There exists $\xi \in (t_0, t)$, which is obtained by using the median theorem of the integral

$$\lambda_i^{(n)}(x,t) - \lambda_i^{(n-1)}(x,t) = \left(\lambda_i^{(n-1)}(x,t) - \lambda_i^{(n-2)}(x,t)\right) + \frac{t}{2} \cdot \frac{2}{t_0^3} \int_{t_0}^{\xi} \left(\lambda_i^{(n-2)}(x,t) - \lambda_i^{(n-3)}(x,t)\right) dt$$

$$= \left(\lambda_i^{(n-1)}(x,t) - \lambda_i^{(n-2)}(x,t)\right) + \frac{t}{t_0^3} \int_{t_0}^{\xi} \left(\lambda_i^{(n-2)}(x,t) - \lambda_i^{(n-3)}(x,t)\right) dt \tag{26}$$

Combining Equation (24) that

$$\left| \frac{t}{t_0^3} \int_{t_0}^{\xi} \left(\lambda_i^{(n-2)}(x,t) - \lambda_i^{(n-3)}(x,t)\right) dt \right| = \left| \lambda_i^{(n)}(x,t) - \lambda_i^{(n-1)}(x,t) - \left(\lambda_i^{(n-1)}(x,t) - \lambda_i^{(n-2)}(x,t)\right) \right|$$

$$\leq \left| \lambda_i^{(n)}(x,t) - \lambda_i^{(n-1)}(x,t) \right| + \left| \lambda_i^{(n-1)}(x,t) - \lambda_i^{(n-2)}(x,t) \right|$$

$$\leq 2Qt \tag{27}$$

Therefore, $\left| \frac{1}{t_0}^3 \int_{t_0}^{\xi} \left(\lambda_i^{(n)}(x,t) - \lambda_i^{(n-1)}(x,t)\right) dt \right|$ is bounded, and let the upper bound of $\left| \lambda_i^{(n)}(x,t) - \lambda_i^{(n-1)}(x,t) \right|$ be S. Then

$$\left| \frac{1}{t_0^3} \int_{t_0}^{\xi} \left(\lambda_i^{(n)}(x,t) - \lambda_i^{(n-1)}(x,t)\right) dt \right| \leq \left| \frac{1}{t_0}^3 S\,(\xi - t_0) \right| = \frac{S(\xi - t_0)}{t_0^3} \tag{28}$$

There exists $L > 0$ such that $\frac{S(\xi - t_0)}{t_0^3} \leq L$, then $S \leq \frac{Lt_0^3}{(\xi - t_0)}$, when $n \to \infty$, $t_0 \to 0$, $S \to 0$, so $\left| \lambda_i^{(n)}(x,t) - \lambda_i^{(n-1)}(x,t) \right| \to 0$, $\lambda_i^{(n)}(x,t)$ converge.

3.3.3 Proof of uniqueness

The following is a proof of uniqueness by contradiction.

Known from 3.3.2, $\lambda_i^{(0)}$ is bounded, $\left| \lambda_i^{(n)}(x,t) - \lambda_i^{(n-1)}(x,t) \right|$ is bounded and $\lambda^{(n)}(x,t)$ converges, so $\lambda^{(n)}(x,t)$ is bounded.

Assuming that the solution of $\lambda_i(x,t)$ is not unique, there exists a bounded function $\mu(x,t)$ that is a solution of $\lambda_i(x,t)$, and there exists $N > 0$ that satisfies

$$\begin{cases} \mu(x,t) = \dfrac{1}{p(t)} \left(I(q(x,t)) + I(\mu(x,t)\dot{p}(t)) - \dot{\lambda}_t(x,t) + \beta_{i0}\bar{R}_{i0} \right) \\ 0 < \left| \mu(x,t) - \lambda_t^{(n)}(x,t) \right| < N \end{cases} \tag{29}$$

Then

$$\mu(x,t) - \lambda_i^{(n)}(x,t) = \frac{1}{p(t)} \left(I(\mu(x,t)\dot{p}(t)) - I\left(\lambda_i^{(n-1)}(x,t)\dot{p}(t)\right) \right)$$

$$= -\frac{t}{2} \int_{t_0}^{t} \frac{2}{t^2} \left(\mu(x,t) - \lambda_i^{(n-1)}(x,t)\right) dt \tag{30}$$

By the integral median theorem, there exists $\zeta \in (t_0, t)$ such that

$$\mu(x,t) - \lambda_i^{(n)}(x,t) = -\frac{t}{2} \int_{t_0}^{t} \frac{2}{t^2} \left(\mu(x,t) - \lambda_i^{(n-1)}(x,t)\right) dt$$

$$= -\frac{t}{t_0^2} \int^{\zeta} \left(\mu(x,t) - \lambda_i^{(n-1)}(x,t)\right) dt \tag{31}$$

Equation (30) deflates to give:

$$N > \left| \mu(x,t) - \lambda_i^{(n)}(x,t) \right| = \left| \frac{t}{t_0^2} \int_{t_0}^{\zeta} \left(\mu(x,t) - \lambda_i^{(n-1)}(x,t)\right) dt \right| \tag{32}$$

Table 1. *Simulation parameterst (normalised)*

	M	D1	D2
Initial position	(0.350,0.180,0.150)	(0.240,0.200,0.050)	(0.100,0.150,0.200)
Initial speed	0.500	0.800	0.667
Initial trajectory angle	0.028	0.014	0.028
Initial trajectory yaw angle	–0.472	0.167	–0.111
Capture radius	0.5c	c	c
Angle-of-attack limit	0.139	0.139	0.139
Overload limit	0.333	1	1

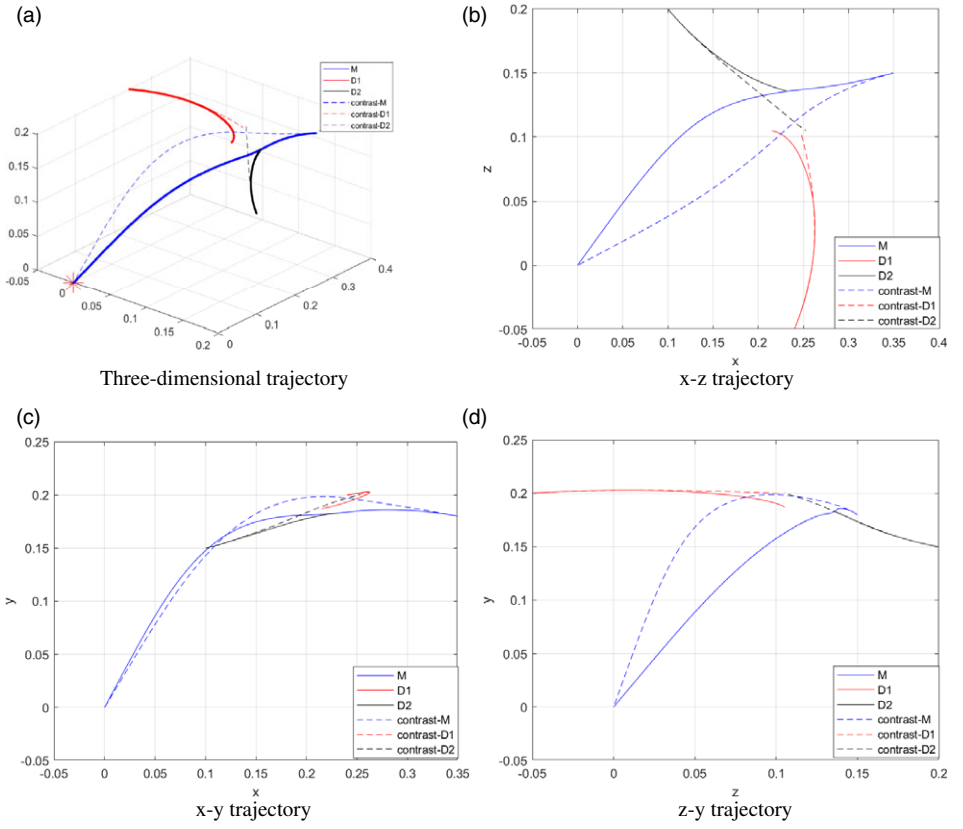

Figure 4. *Comparison of experimental trajectories with method 1.*

Let $0 < L \leq N$, L is the lower bound of $\left(\mu(x,t) - \lambda_i^{(n-1)}(x,t)\right)$. So when $n \to \infty$, there are

$$\left|\mu(x,t) - \lambda_i^{(n)}(x,t)\right| = \left|\frac{t}{t_0^2}\int_{t_0}^{\zeta}\left(\mu(x,t) - \lambda_i^{(n-1)}(x,t)\right)dt\right| \geqslant \frac{Lt(\zeta - t_0)}{\substack{2\\0}} \tag{33}$$

Therefore

$$L \leq \frac{Nt_0^2}{t(\zeta - t_0)} \tag{34}$$

When $n \to \infty$, $t_0 \to 0$, $t_0 < t < t_{fj}$, then $L \to 0$, which contradicts $0 < L \leq N$. Therefore, the assumption is not valid and the solution of $\lambda_i(x,t)$ is unique.

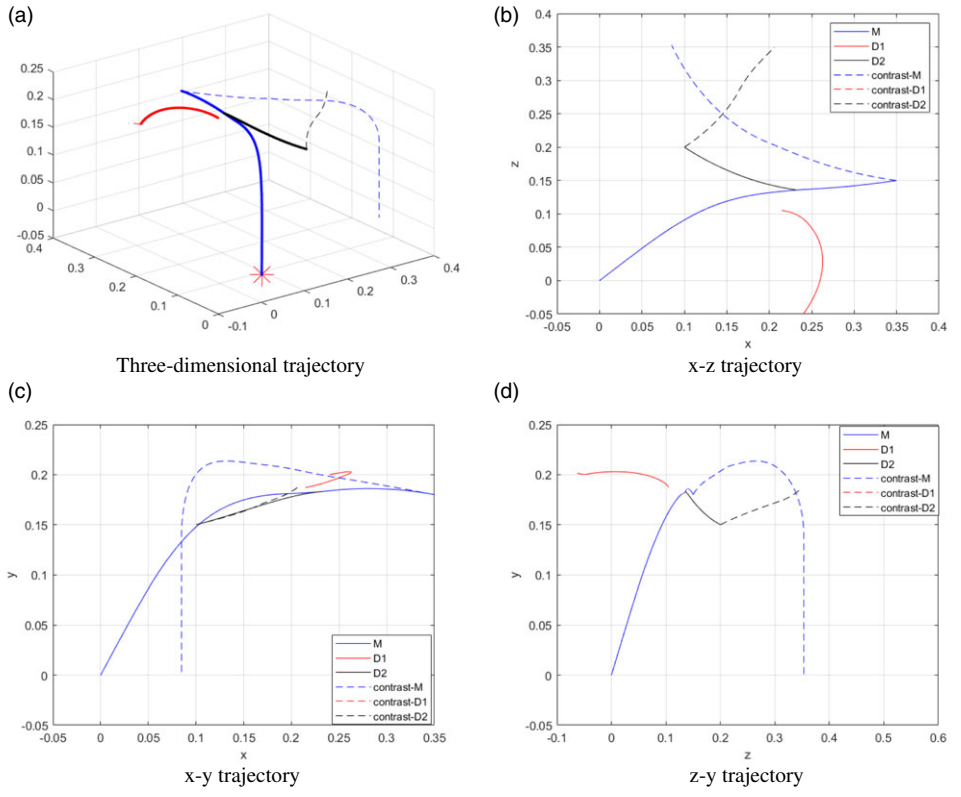

Figure 5. *Comparison of experimental trajectories with method 2.*

This section details the development of an optimal avoidance strategy for UAVs based on a nonlinear dynamical model. It demonstrates the convergence and uniqueness of the key variables, known as covariates, within this strategy. Consequently, the proposed approach offers a rigorously validated solution to the nonlinear optimal strategy, addressing the shortcomings of traditional analytical methods. This advancement holds significant implications for improving UAV evasion tactics.

4.0 Simulation results and comparison

4.1 Simulation condition

The simulation experiment uses the non-cooperative differential game given in this paper for a game scenario with two pursuers $D1$, $D2$ and one escapee M. The simulation stops when the escapee evades pursuit and reaches the destination. Or, it stops if the escapee is not pursued. The shooting plane energy metrics are weighted $\kappa_D = 10$, and the horizontal plane energy metrics are weighted $\kappa_T = 100$. The destination is set at the origin (0, 0, 0), and c is a constant. The simulation parameters are set as in Table 1.

4.2 Simulation results

The escapee M uses the strategy designed in this paper, and the pursuers $D1$ and $D2$ use proportional guidance. Under Table 1, the evasion is successful, M evades 112.633c against $D1$, and 2.533c against $D2$. The final distance between M and T is 0.133c, the final velocity of M is 0.192, and the time when M reaches T is 44.180.

According to the Apollo circle method described in reference (33), as method 1, the comparison experiment involving escaping with optimal avoidance strategy is conducted. The simulation yielded

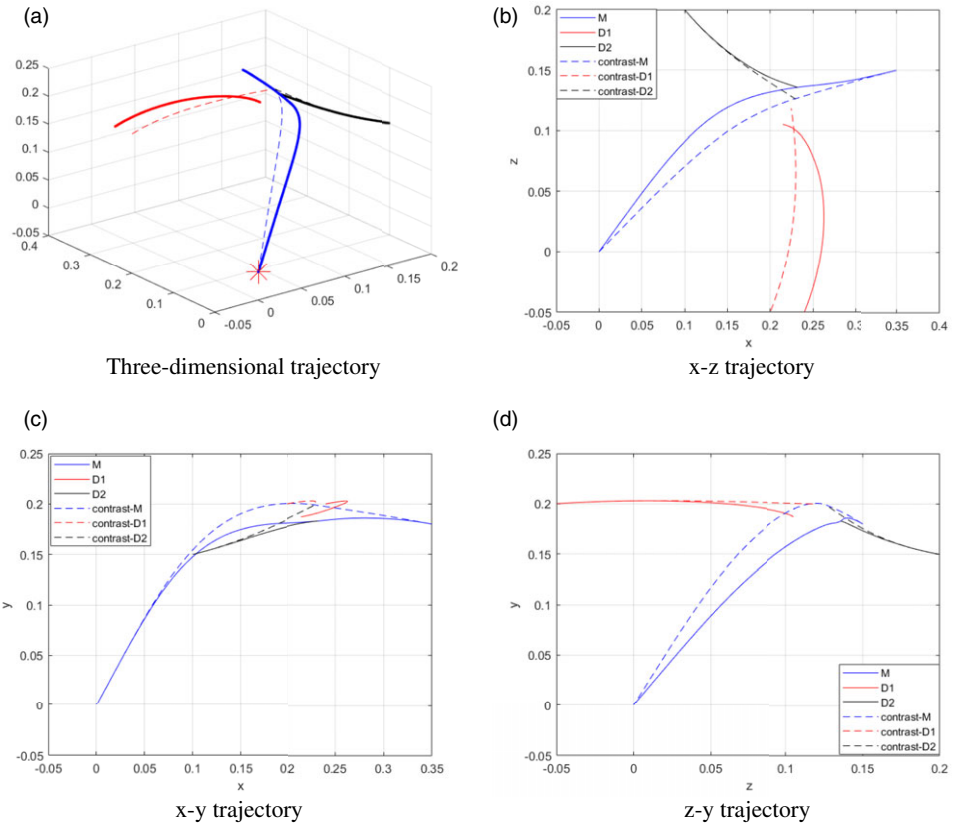

Figure 6. *Comparison of experimental trajectories with method 3.*

successful results, reaching the destination and M escaping against $D1$ 49.366c and $D2$ 1.067c. The final distance between M and T was 0.2376c, while M's final velocity was 0.190, and it took 73.600s for M to reach T.

According to the method using lift coefficients as control quantities, as method 2, described in reference (6), the comparison experiment involving escaping with optimal avoidance strategy is conducted. M only succeeds in avoidance but not reaching T, and M escaping against $D1$ 226.342c and $D2$ 765.333c. The final distance between M and T was 30c.

According to the method based on a dynamic multi-objective algorithm, as method 3, described in reference (34), the comparison experiment involving escaping with optimal avoidance strategy is conducted. The simulation yielded successful results, reaching the destination and M escaping against $D1$ 1.027c and $D2$ 1.816c. The final distance between M and T was 0.333c, while M's final velocity was 0.160, and it took 200.600s for M to reach T.

The trajectories are shown in Figs 4, 5 and 6, where M is the escapee's trajectory and $D1$ and $D2$ are the pursuers' trajectories. The dashed line shows the control experiment, contrast-M is the escapee's trajectory, contrast-$D1$ and contrast-$D2$ are the pursuers' trajectories.

Through the analysis depicted in Figs 4–6, it is evident that the optimal avoidance strategy delineated in this study surpasses the methodology expounded in the existing methods. This superiority is demonstrated by the heightened efficacy in enabling entity M to more adeptly evade the pursuers $D1$ and $D2$. Subsequent to the successful evasion, M systematically employs the optimal avoidance strategy to navigate towards the target point T. Using this method greatly reduces the final distance between M and T. It also cuts the task completion time. The final speed greatly rises with the best avoidance strategy. These results highlight the strategy's high effectiveness and superiority.

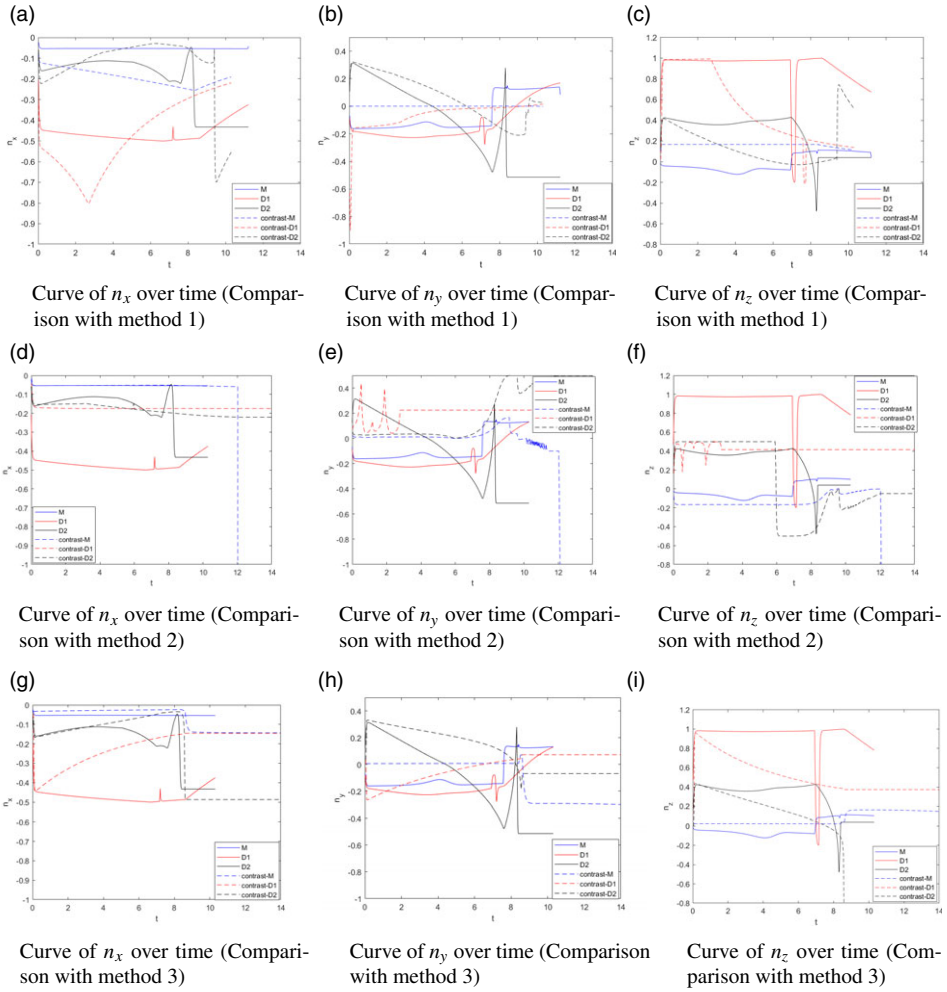

Curve of n_x over time (Comparison with method 1)

Curve of n_y over time (Comparison with method 1)

Curve of n_z over time (Comparison with method 1)

Curve of n_x over time (Comparison with method 2)

Curve of n_y over time (Comparison with method 2)

Curve of n_z over time (Comparison with method 2)

Curve of n_x over time (Comparison with method 3)

Curve of n_y over time (Comparison with method 3)

Curve of n_z over time (Comparison with method 3)

Figure 7. *Overload variation curve.*

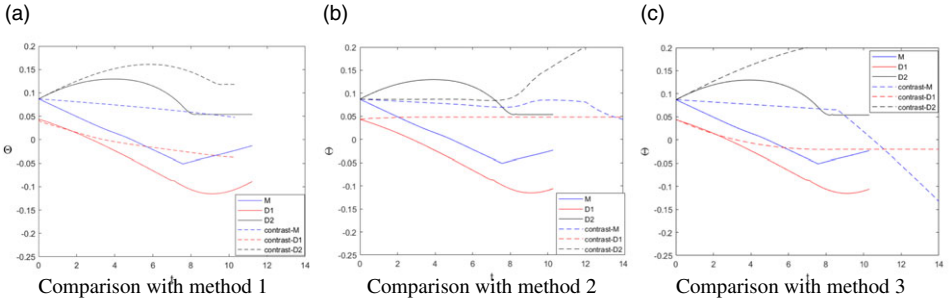

Comparison with method 1

Comparison with method 2

Comparison with method 3

Figure 8. *Track angle variation curve.*

Figures 7–10 serve as visual representations of the simulated outcomes arising from the evasion process for both the proposed optimal avoidance strategy and the control group experiment, denoted by the dashed line. The simulation results distinctly illustrate that the optimal avoidance strategy delineated in this study empowers entity M to execute manoeuvers of heightened versatility, characterised by a smaller angle-of-attack, able to efficiently complete the escape to reach T.

Table 2. *Intrusion process interference settings*

Serial number	Restraint	$\sigma 3$
1	Initial speed (%)	10
2	Initial trajectory angle	0.2
3	Initial trajectory yaw angle	0.2
4	Initial height (%)	10
5	Pneumatic coefficient (%)	5
6	Atmospheric density (%)	5

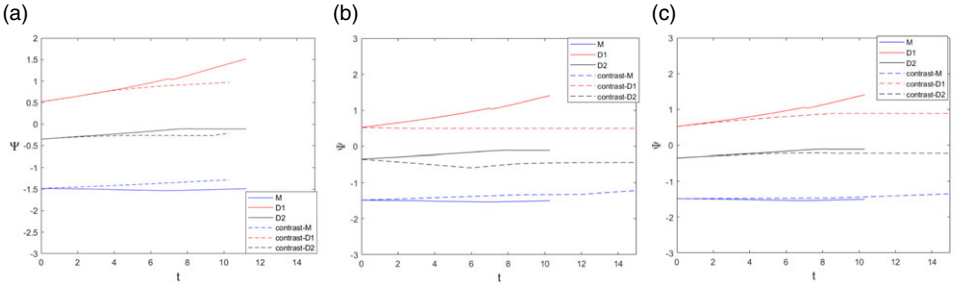

Comparison with method 1 Comparison with method 2 Comparison with method 3

Figure 9. *Track yaw angle variation curve.*

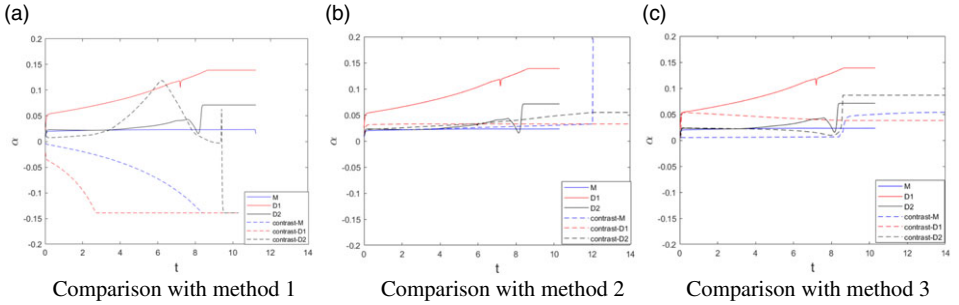

Comparison with method 1 Comparison with method 2 Comparison with method 3

Figure 10. *Angle-of-attack variation curve.*

In order to test the effectiveness of the optimal avoidance strategy proposed in this paper, we conducted 1,000 anti-jamming simulation experiments [35]. We establishes a Gaussian distribution of the interference factors and recorded the results in Table 2. During the experiments, we observes that M's evasion against $D1$ ranged from 128.133c to 90.233c, while M's evasion against $D2$ ranged from 2.699c to 1.911c. These distances are greater than the capture radius of the pursuer, indicating that M was able to evade successfully in all 1,000 experiments.

During the experiments, we observes that M's evasion against $D1$ ranged from 128.133c to 90.233c, while M's evasion against $D2$ ranged from 2.699c to 1.911c. These distances are greater than the capture radius of the pursuer, indicating that M was able to evade successfully in all 1,000 experiments.

The results of the experiment are depicted in Figs 11–13. These figures demonstrate that the non-cooperative differential game optimal avoidance strategy is robust enough to meet different constraints, even in the presence of disruptive factors.

In comparison, methods 1 and 2 have poor robustness, while method 3 has a 30% probability of successful escape and has no comparative value, so no graphs are shown.

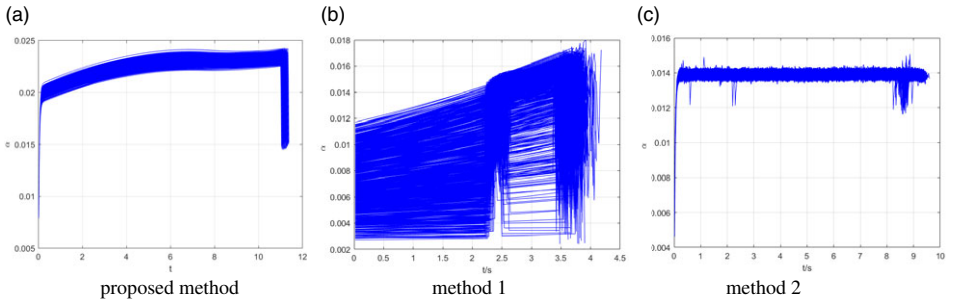

Figure 11. *Angle-of-attack variation curve.*

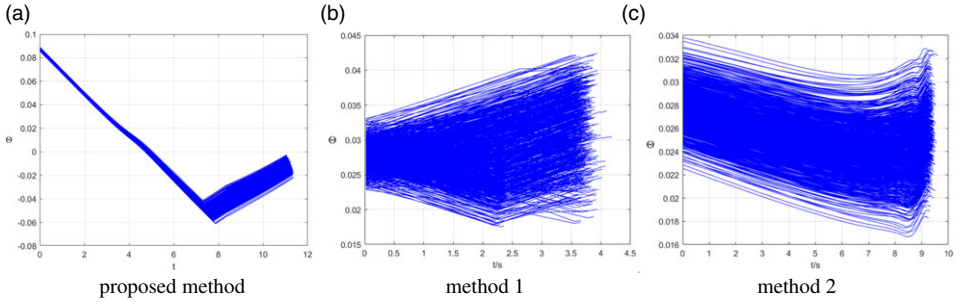

Figure 12. *Track angle variation curve.*

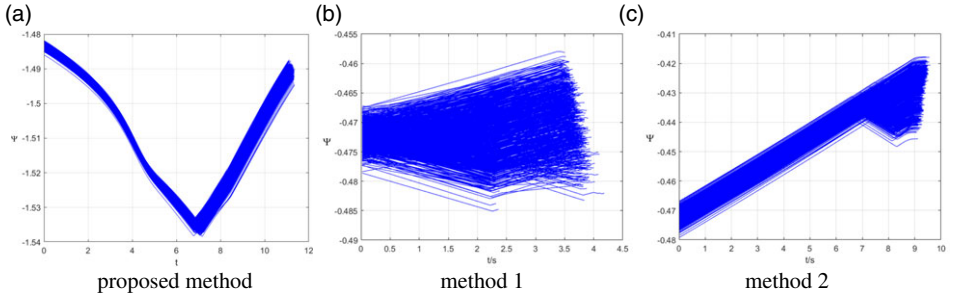

Figure 13. *Track yaw angle variation curve.*

The simulation comparison indicates that for the 'two pursuing one' UAV pursuit-evasion scenario, the proposed method in this paper excels in evading pursuit and conserving energy. It also demonstrates strong robustness under various interferences. In three-dimensional simulations, the method shows significant potential for engineering applications.

5.0 Conclusion

In response to the challenge posed by UAVs pursuit-evasion scenarios, this paper presents an optimal avoidance strategy based on non-cooperative differential game theory. Embracing the intricate dynamics inherent to UAVs, this strategy is tailored for practical multi-vehicle game scenarios, leveraging a three-degree-of-freedom nonlinear dynamic model. A pivotal aspect of this investigation entails the analytical resolution of nonlinear HJB equations. This analytical solution is attained via the Cauchy initial value problem, with its convergence and uniqueness meticulously proofed. Comparative analysis juxtaposes the simulation outcomes of the proposed optimal evasion strategy against those of three

traditional advanced game strategies. The results unequivocally highlight the superior efficacy of the proposed strategy in evasion manoeuvers, accompanied by notable energy conservation. Subsequently, systematic anti-jamming simulation experiments are conducted to validate the viability and robustness of the proposed evasion strategy under diverse uncertainties. Demonstrating applicability and effectiveness, in scenarios where the pursuer possesses superior capabilities to the evading party, this strategy holds promise in addressing UAV pursuit-evasion dynamics. The insights gleaned from this study enrich the discourse surrounding the avoidance of moving obstacles and adept pursuers by UAVs, pertinent to dynamics of real-world UAV operations.

Funding statement. The authors did not receive support from any organisation for the submitted work.
No funding was received to assist with the preparation of this manuscript.
No funding was received for conducting this study.
No funds, grants or other support was received.

References

[1] Weintraub, I., Pachter, M. and Garcia, E. An introduction to pursuit-evasion differential games, 2020 American Control Conference (ACC), IEEE, 2020.
[2] Liu, Y., Qi, N. and Wang, T. Capture condition for endo-atmospheric interceptors steered by alcs and arcs, *Control Theory Technol.*, 2014, **12**, (1), pp 56–67.
[3] Vrabie, D. and Lewis, F. Adaptive dynamic programming for online solution of a zero-sum differential game, *J. Control Theory Appl.*, 2011, **9**, (3), pp 353–360.
[4] Perelman, A., Shima, T. and Rusnak, I. Cooperative differential games strategies for active aircraft protection from a homing missile, *J. Guid. Control Dyn.*, 2011, **34**, (3), pp 761–773.
[5] Shaferman, V. and Shima, T.Y. A cooperative differential game for imposing a relative intercept angle, *AIAA Guidance, Navigation, and Control Conference*, 2017, p 1015.
[6] Liang, H., Li, Z., Wu, J., Zheng, Y., Chu, H. and Wang, J. Optimal guidance laws for a hypersonic multiplayer pursuit-evasion game based on a differential game strategy, *Aerospace*, 2022, **9**, (2), p 97.
[7] Garcia, E., Casbeer, D.W. and Pachter, M. Design and analysis of state-feedback optimal strategies for the differential game of active defense, *IEEE Trans. Autom. Control*, 2018, **64**, (2), pp 553–568.
[8] Kang, Y., Yu, J., Dong, X. and Ren, Z. Cooperative differential games guidance laws for multiple missiles against an active defense target with multiple defenders, *International Conference on Guidance, Navigation and Control*, Springer, 2022, pp 4601–4610.
[9] Pachter, M., Garcia, E. and Casbeer, D.W. Active target defense differential game, *2014 52nd Annual Allerton Conference on Communication, Control, and Computing (Allerton)*, IEEE, 2014, pp 46–53.
[10] Zhang, H., Zhang, Y. and Zhang, P. Optimal guidance law for intercepting the active defense aircraft with terminal angle constraint, *J. Phys. Conf. Ser.*, 2021, 1828, (1), p 012160 (15 pp).
[11] Li, Y. and Qi, N. Logic-based guidance law for interceptor missiles steered by aerodynamic lift and divert thruster, *IEEE Trans. Control Syst. Technol.*, 2011, **19**, (4), pp 884–890.
[12] Humin, L., Xu, Z., Feiyao, D. and Jiong, L.I. Finite time convergent zero-effort miss guidance law, *J. Natl. Univ. Def. Technol.*, 2015, **37**, (3), pp 136–141.
[13] Liwei, Z., Wuxing, J. and Jianying, Z. [IEEE 2007 Chinese Control Conference - zhangjiajie, china (2007.07.26-2007.06.31)] 2007 Chinese Control Conference - Zero Effort Miss Formulation for Longer Range Targeting, 2006, pp 414–417.
[14] Su Shan, B.Y.L.Y., Yongjie, X. and Yongzhi, S. Research on cooperative countermeasure guiding law methods for differential countermeasures, *Air Space Def.*, 2022, 002, pp 58–64.
[15] Weintraub, I., Garcia, E. and Pachter, M. Optimal guidance strategy for the defense of a non-manoeuvrable target in 3-dimensions, *IET Control Theory Appl.*, 2020, **14**, (11), pp 1531–1538.
[16] Yan, R., Shi, Z. and Zhong, Y. Reach-avoid games with two defenders and one attacker: An analytical approach, *IEEE Trans. Cybern.*, 2018, **49**, (3), pp 1035–1046.
[17] Bakolas, E. and Tsiotras, P. Optimal pursuit of moving targets using dynamic voronoi diagrams, *IEEE Conference on Decision and Control*, Atlanta, GA, IEEE, 2010, pp 7431–7436.
[18] Zhou, Z., Zhang, W., Ding, J., Huang, H., Stipanovicć, D.M. and Tomlin, C.J. Cooperative pursuit with voronoi partitions, *Automatica*, 2016, **72**, pp 64–72.
[19] Chipade, V.S. and Panagou, D. Multiplayer target-attacker-defender differential game: Pairing allocations and control strategies for guaranteed intercept, *AIAA Scitech 2019 Forum*, 2019, p 0658.
[20] Coon, M. and Panagou, D. Control strategies for multiplayer target-attacker-defender differential games with double integrator dynamics, *2017 IEEE 56th Annual Conference on Decision and Control (CDC)*, IEEE, 2017, pp 1496–1502.
[21] Makkapati, V.R. and Tsiotras, P. Optimal evading strategies and task allocation in multi-player pursuit–evasion problems, *Dyn. Games Appl.*, 2019, **9**, pp 1168–1187.

[22] Ninyu, W., Shan, S., Naigang, C., Yongzhi, S. and Shengli, X. Multi-vehicle cooperative optimal allocation method based on differential countermeasures, *Tactical Missile Technol.*, 2021, 6, pp 130–138.
[23] Wei, X. and Yang, J. Optimal strategies for multiple unmanned aerial vehicles in a pursuit/evasion differential game, *J. Guid. Control Dyn. A Publ. Am. Inst. Aeronaut. Astronaut. Devoted Technol. Dyn. Control*, 2018, **41**, (8), pp 1798–1805.
[24] Chen, S. and Li, X. Viscous solutions of the Hamilton-Jacobi equation discounted on a non-tight space, *J. East China Normal Univ. Nat. Sci. Ed.*, 2022, (002).
[25] Kawohl, B. and Kutev, N. A study on gradient blow up for viscosity solutions of fully nonlinear, uniformly elliptic equations, *Acta Math. Sci.*, 2012, **32**, (1), pp 15–40.
[26] Wang, K. Exponential convergence to time-periodic viscosity solutions in time-periodic hamilton-jacobi equations, *Chin. Ann. Math. Ser. B*, 2018, **39**, (1), pp 69–82.
[27] Li, X. and Yan, J. Weak kam theory and Hamilton-Jacobi equations, *Sci. Sinica Phys. Mech. Astron.*, 2014, **44**, (12), p 1286.
[28] Hamadène, S. Mixed zero-sum stochastic differential game and american game options, *SIAM J. Control Optim.*, 2006, **45**, (2), pp 496–518.
[29] Chen, C., Wang, Y.-N. and Yan, J. Convergence of the viscosity solution of non-autonomous hamilton-jacobi equations, *Sci. China Math.*, 2021, **64**, pp 1789–1800.
[30] Xing, G. Research on hypersonic vehicle game breaching strategy, PhD dissertation, Northwestern Polytechnical University.
[31] Bressan, A. and Shen, W. Small bv solutions of hyperbolic noncooperative differential games, *SIAM J. Control Optim.*, 2004, **43**, (1), pp 194–215.
[32] Youness, E.A., Megahed, A.E.-M.A., Eladdad, E.E. and Madkour, H.F. Min-max differential game with partial differential equation, *AIMS Math.*, 2022, **7**, (8), pp 13777–13789.
[33] Makkapati, V.R., Sun, W. and Tsiotras, P. Pursuit-evasion problems involving two pursuers and one evader, *2018 AIAA Guidance, Navigation, and Control Conference*, 2018, p 2107.
[34] Zheng-Ping, L., Hui-Cai, L., Zhi-Qiang, W., Kai-Feng, H. and Ze-Xuan, Z. Dynamic multi-objective evolutionary algorithm with adaptive change response, *Acta Automatica Sinica*, 2023, **49**, (8), pp 1688–1706.
[35] Zhou Hongyu, S.Y.Z.Y.C.N. and Xiaogang, W. Cooperative trajectory planning for aircraft based on improved particle swarm algorithm, *J. Automat.*, 2022, **48**, pp 2670–2676.

Cite this article: Zhao S.J., Zhang H.R., Lyu R., Yang J. and Xue C.C. Optimal avoidance strategy based on nonlinear approximate analytic solution of non-cooperative differential game. *The Aeronautical Journal*, https://doi.org/10.1017/aer.2024.61